

A finite element solution of the Reynolds equation of lubrication with film discontinuities: application to helical groove seals

M Jarray, D Souchet, Y Henry and A Fatu

Institut Pprime, Université de Poitiers CNRS– ISAE-ENSMA - UPR 3346 SP2MI -
Téléport 2 - 11 Boulevard Marie et Pierre Curie, BP 30179 F86962 Futuroscope
Chasseneuil Cedex, Poitiers, France

E-mail: mohamed.jarray02@univ-poitiers.fr

Abstract. Helical groove seal, is one of the very few non-contact seals that have the capability to effectively seal a liquid. It finds use mainly in turbines and compressors. Although its reliability, this type of seals has not been investigated thoroughly because of its complex characteristics. This work presents a numerical analysis of a helical groove seal operating in laminar regime by means of solving the Reynolds equations for incompressible fluid film in steady state. Equations governing the fluid flow were solved by the finite element method.

Although the simplifying assumptions of Reynolds model help to keep the computational time at an acceptable level, the inertia effects are neglected which may lead to unreliable results especially where the film thickness is discontinuous. The present approach, inspired by Arghir *et al.* [1] is able to take into account concentrated inertia effects, as described by a generalized Bernoulli equation. Comparisons made with the classical Reynolds model show that the film discontinuities should be taken into account when dealing with helically grooved seals. In addition, the leakage of fluid towards the air side was investigated for different parameters such as the groove angle and depth.

1. Introduction

Although the limited studies on helically grooved seals, also known as viscoseals, that have been carried out during the past decades, some theories related to the flow in the helical seal channel have been developed, however, applying these theories to the helical grooves design has not been entirely accurate. The main reason is that they rely on a number of simplifying assumptions that lead to the celebrated Reynolds equation, which is not accurate enough for some cases, such high Reynolds number flow or a sudden change in geometry at the edge of the grooves causing film discontinuity, where the inertia effects and the energy loss can't be neglected [2].

The first study to mention a net pressure gain resulting from inertia effect was presented in 2003 by Argir *et al.* [3] By means of a computational fluid dynamics (CFD) analysis of a single macro-roughness, the authors concluded that the inertia effect is present for Re numbers larger than 1. Later in 2005, the suitability of a Reynolds-based method in analyzing discontinuous film thickness domains started to be discussed, Dobrica and Fillon [4] presented a study comparing a Reynolds-based numerical model and the Navier-Stokes model. The models were solved for a 2D geometry of a Rayleigh step. It was shown that, as long as the film thickness remains small, below 120 μm , the two



methods give close results, with less than 3% difference. Subsequently, Sahlin *et al.* [5] Investigated the inertia effects in single texture configurations by mean of a 2D CFD analysis on parallel sliding contacts with circular and splined grooves. They reported that the effects of inertia were the dominant mechanism for pressure build-up and load carrying capacity. Their results indicated that load support increases with increase in Reynolds number and groove width. However, four years later, completely contrary results were presented by Dobrica and Fillon [2]. They investigated the domain limit where the Reynolds equation is valid by mean of 2D CFD study on an elementary texture cell, where the texture density and dimple depth to land film thickness are kept constant, they found that inertia in general has a negative effect on the load carrying capacity. Furthermore, it was shown that Reynolds equation is applicable in many practical configurations and that the texture aspect ratio $\lambda = l_d/h_d$ (ratio between the length of the dimple and its depth) is equally important in determining the validity of Reynolds equation, they noted also that, for small λ ratios (less than ~ 10), the Re model is inapplicable whatever the Reynolds number. It is noteworthy that Dobrica and Fillon stated in [2] that the inertia effects introduced by the dimple are quite similar to those observed in Rayleigh step bearings, and hence such inertia effects can be partially corrected in the region of discontinuous fluid film thickness, by means of the method used by Arghir *et al.* [1] based on equation (2), and therefore if added to the Reynolds equation, it extends the validity domain of a Reynolds-based models.

Another key issue that was the focus of a great deal of research efforts on lubrication was the treatment of cavitation phenomena on textured surfaces, as it is responsible of rupture of the lubricated film and may occur multiple times. A mass-conservative treatment of cavitation has been shown to be crucial for accurate performance predictions. Many cavitation algorithms based on Finite element method (FEM) were developed during the last decades [6] [7], and in the early 2000s, Hajjam and Bonneau [8] [9] used a modified version of the Reynolds equation, and introduced a single variable from which the fields of the pressure and a complementary variable are reconstructed. Their model was recently applied for the study of textured parallel sliders under steady and transient conditions by Gherca *et al.* [10]. Hajjam and Bonneau formulation was later used by Fatu *et al.* [11] [12] [13] for the study of dynamically loaded bearings and by Targaoui *et al.* [14], who investigated viscoelastic's optimal geometrical and operating conditions. There are few other studies that aimed to analyze the flow characteristics and operating conditions of helical groove seals, for instance, Kanki and Kawakami [15] studied the leakage characteristics of helically grooved seals and reported that the leakage flow of the viscoelastic was less than that of the plain seal. Ludwig *et al.* [16] analyzed the effect of helical profile of the seal on the pressure distribution, and determined that each groove-land pair repeats the same pressure pattern and provides a saw-tooth pressure profile around the circumference of the seal. In this paper, considering Ludwig *et al.* results, a periodic boundary condition will be applied at the boundary of the groove-land domain, additionally, Hajjam and Bonneau's cavitation treatment method is considered.

The aim of this work is to explore the possibility of predicting, numerically, the flow behavior in a helically grooved seals using a developed Finite Element code adopting the seal unwrapping approach, and considering, both, the modified Reynolds equation of cavitation model by Hajjam and Bonneau and the inertia correction based on the method used by Argir *et al.* [1]. The results are compared with the Reynolds only model and Navier-Stokes model using OpenFoam CFD Code. The leakage of fluid towards the air side is investigated for different helical groove parameters, such as groove angle and depth.

2. Problem definition and modeling approach

The problem to be considered is that of a helically grooved seals with a groove angle β , clearance h_f , and groove length to depth aspect ratio λ . A common approach for modelling flow in the helical channel is to unwrap the channel from the seal [14]. However the unwrapping in our case is inclined in such a way that the flow domain will be viewed as a flat grooved plate inclined by an angle β , the helix angle relative to the normal to the flow entrance, as depicted in Figure 1. Helicity and curvature effects are neglected by the unwrapping procedure. In fact, this method is only valid for helical grooves channels with clearance relatively very small compared with the seal radius, as demonstrated in the work of Dai *et al.* [17] who numerically evaluated the influence of the film curvature on the pressure, and noted a slight difference, between the original polar coordinates system representation

and the simplified flattened Cartesian system representation, that tend to disappear when the clearance to radius ratio h_f/R approaches zero.

2.1. Governing Equations

The analytical formulation for cavitation treatment adopted in this paper is detailed in the work of Hajjam and Bonneau [8] and consists of the use of a modified version of the Reynolds equation, which can be applied throughout the entire domain, both in the cavitated and the non-cavitated regions. It can be written as follows

$$F \left\{ \frac{\partial}{\partial x} \left(\frac{h^3}{12\mu} \frac{\partial D}{\partial x} \right) + \frac{\partial}{\partial z} \left(\frac{h^3}{12\mu} \frac{\partial D}{\partial z} \right) \right\} = \frac{1}{2} U \frac{\partial h}{\partial x} + \left\{ \frac{1}{2} U \frac{\partial D}{\partial x} \right\} (1 - F) \quad (1)$$

where, in the active region

$$\begin{cases} D = p - p_{cav} \\ F = 1 \end{cases}$$

and in the inactive region

$$\begin{cases} D = r - h \\ F = 0 \end{cases} \text{ where } r = \frac{\rho}{\rho_0} h$$

p_{cav} is the cavitation pressure, considered constant in the cavitation zone and h the film thickness.

The correction for inertia effects was introduced in the Modified Re model. The procedure leading to the Modified Re model with inertia correction (Re+I) is detailed in reference [18], and it is based on equation (2), written here for a discontinuity in the film thickness in the x -coordinates

$$p(x^-) + \frac{\rho(u(x^-))^2}{2} = p(x^+) + \frac{\rho(u(x^+))^2}{2} + \xi \frac{\rho[\text{MAX}(u(x^-), u(x^+))]^2}{2} \quad (2)$$

where the coordinates x^+ and x^- denote the locations found immediately upstream and downstream of the discontinuity, ξ pressure drop coefficient and u denotes the fluid velocity.

2.2. Modeling approach

For the finite element approach, a viscoseal of four grooves is considered, with clearance to radius ratio of 0.00625 and film thickness h accorded along the y -axis. The computational domain is assumed to be a two dimensional rectangular surface unwrapped from the cylindrical seal form by cutting it in the same direction as the grooves edge, and in which an uniform Cartesian mesh of $N_x \times N_z$ nodes is defined, with space of $x_i = I/N_x$ and $z_i = L/N_z$ where $N_1 = 32$ and $N_2 = 320$. A finite element algorithm is adopted to solve the governing equations, it have the advantage to easily deal with domains of complex geometry where grooves or discontinuities are located on seal faces, so the difficulties due to film thickness discontinuities can be also avoided.

The following boundary conditions and assumptions are made in the present work.

- A fixed pressure is set at the inlet and the outlet, one side maintained at atmospheric pressure and the other side at higher pressure of 0.3 MPa.
- The inclined sides are set as periodic boundary conditions.
- Steady state operation is assumed.
- The flow is laminar and the sealed fluid is ISO VG 46 with a constant dynamic viscosity of $\mu = 0.045$ Kg/m.s and density $\rho = 900$ kg/m³.

A grid-independence analysis was carried out before each simulation to achieve the independence of the mesh from pressure distribution and hence ensure the accuracy of the numerical results.

For Navier-Stokes (NS) calculations, a 3D geometry of the flow domain of the seal texture is created (figure 1) where L is the seal length and I_d the groove length, the domain is meshed with structured hexahedron cells totaling 1838585 nodes, with 13 nodes at the clearance zone in y -direction, 241 in x -direction, and 401 nodes along the z -direction (figure 2). The simpleFoam solver of the OpenFOAM packages was used, which is a steady-state solver for incompressible fluids employing the finite volume method. The same fluid properties and boundary conditions as in the Re+I case were used in OpenFoam.

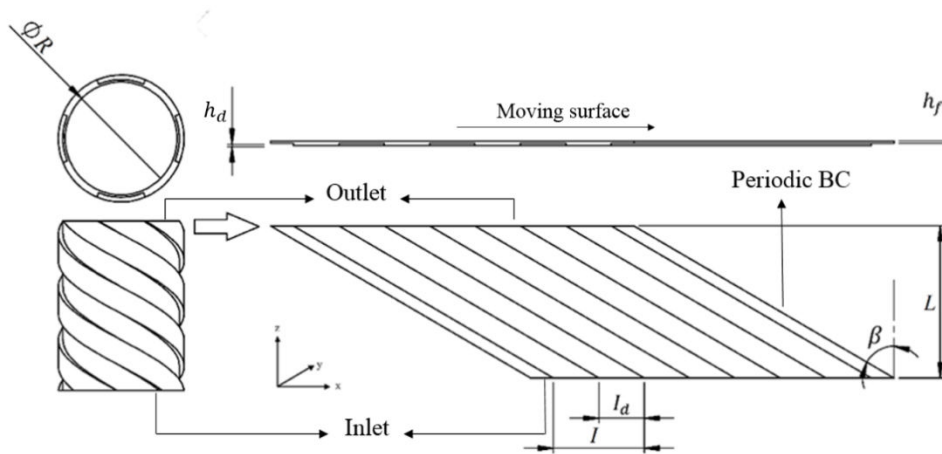


Figure 1. Flatted hellically grooved seal with 4 grooves.

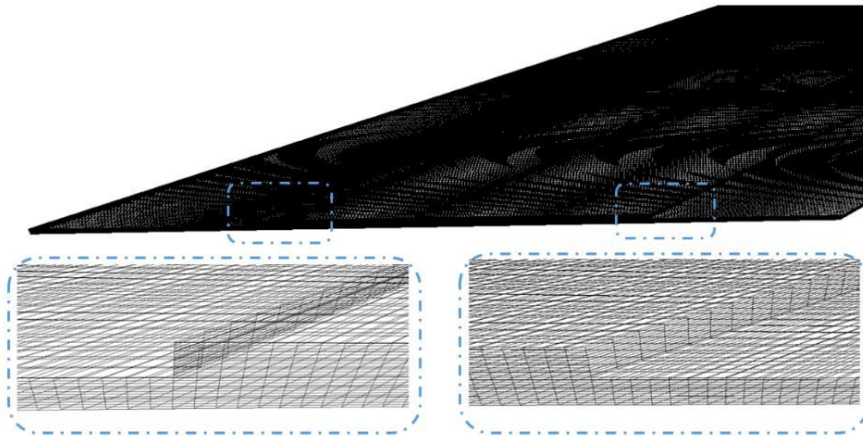


Figure 2. Close-up views of the 3D mesh.

3. Results and discussions

A significant number of numerical simulations were conducted, using either, the Modified Re+I code or the CFD simulation software (OpenFoam), for all ranges of Reynolds number.

A comparison between flatted and non-flatted geometry using NS model by mean of CFD code OpenFoam is presented in figure 3, where the pressure along x-axis at distance $z/L=0.5$ from the seal inlet, is shown. It can be seen that the pressure distribution in both, the grooved (a) and the ungrooved (b) faces, for flatted and cylindrical geometry, have almost the same profile.

An example of test configuration for flatted and non-flatted geometry obtained using OpenFoam is provided for illustrative purpose in figure 4.

The accuracy of the Re + I code was evaluated by comparing it with the NS results obtained using OpenFoam. Figure 5 shows the linear dimensionless pressure distributions along x-axis at $z/L=0.5$ for different Reynolds number ranging from 10 to 40, and based on hydraulic diameter of the seal inlet (equation 3 and 4).

$$Re = \frac{\rho v D_h}{\mu} \quad (3)$$

where v is the linear velocity of the outside surface and D_h the hydraulic diameter at the inlet, which is equivalent to the ratio of 4 times the inlet area to the wetted perimeter:

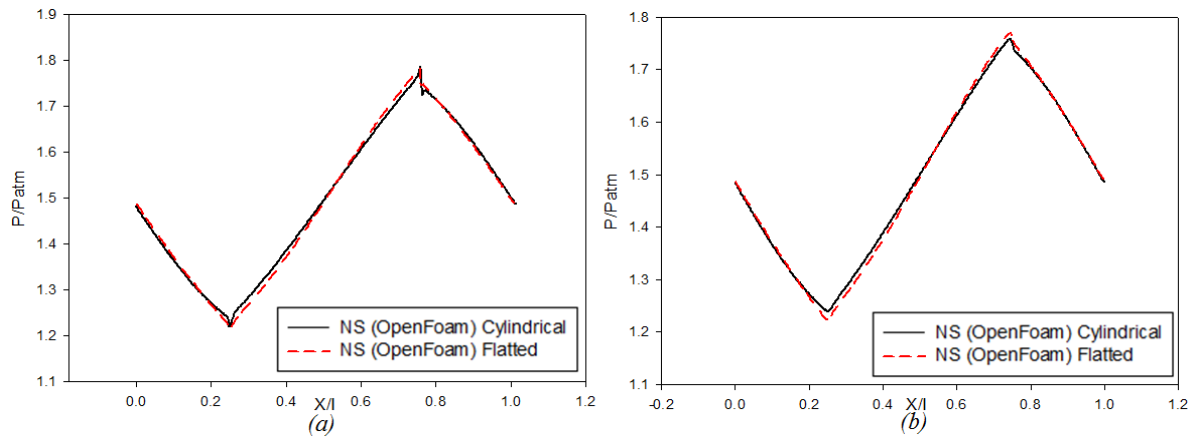


Figure 3. Pressure along x axis at z/L=0.5 for grooved face (a) and ungrooved face (b).

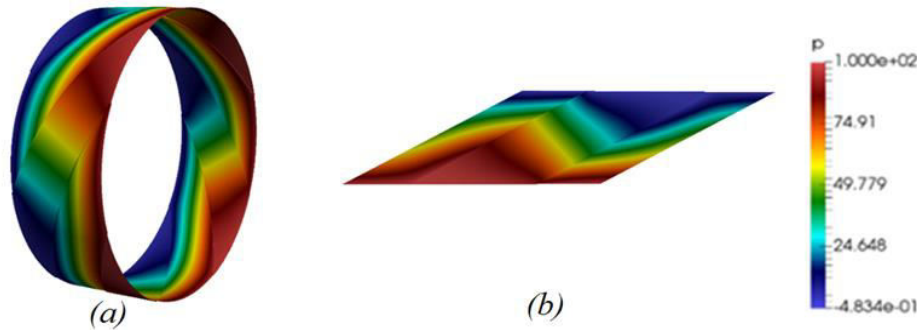


Figure 4. Pressure distribution obtained using OpenFoam: non-flatted seal (a) and flatted seal's cell (b).

$$D_h = 4 \frac{I \cdot h_f + I_d \cdot h_d}{2(I + h_d)} \tag{4}$$

where h_d is the groove depth as depicted in figure 1. The results show that the seal geometry significantly affects the pressure distribution, as the developed pressure starts to increase at the start of the groove and decreases sharply at its end. A close-up view at the film discontinuity zone is presented for each case (figure 5 (a) and (b)). It is clear that Re+I and NS have nearly the same profile with a maximum relative error located around the film discontinuity zone, which does not exceed 0.01 for all cases. The relative error is the ratio of the absolute difference between the NS and Re+I model pressure values at x-coordinate, and the value obtained with NS model.

$$e_r = \frac{|P_{NS}(x) - P_{Re+I}(x)|}{|P_{NS}(x)|} \tag{5}$$

However for Reynolds only model, it is clear that the relative error is slightly more important which can be explained by the fact that Reynolds equation does not take into account the inertia effect. It is also noticeable that, for bigger Reynolds number, Re+I tends to overestimate the pressure loss at the discontinuity zone (a) where the groove ends, and where the relative error $e_r \approx 0.01$.

The effect of groove length to depth aspect ratio λ on the leakage, obtained using the Modified Re+I model for different rotational speed ranged from 500 rpm to 2000 rpm is shown in Figure 6a. The leakage distance z/L is the wetted distance, starting from the inlet, divided by seal length. It can be seen that for all rotational speeds, the leakage increases with the increase of λ ; furthermore it is clear that the leakage becomes more sensitive to rotational speed, as the ratio λ increases.

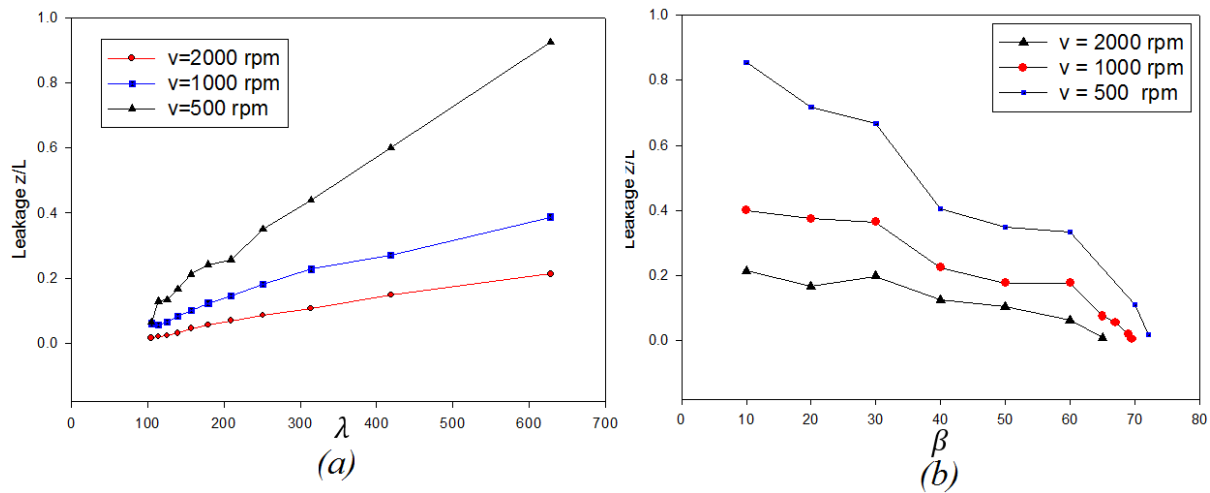


Figure 6. Leakage as function; of groove length to depth aspect ratio λ (a) and of helix angle (b).

Figure 6b shows the leakage distance for different helix angles. As it can be seen, the helically grooved seal, seals better as the helix angle β increases until reaching an optimal sealing angle situated between 65° and 75° for which the leakage distance is minimum, because the seal with a bigger helix angle has more axial component flow and longer groove in favor of energy dissipation. Furthermore fluid rotation opposes the helix angle, and it yields to a reduction of the average circumferential fluid velocity. This is in line with what has been found in previous works carried out for Re model [14].

4. Conclusion

The aim of this article is to summarize a methodology that numerically solve hydrodynamic lubrication problems on helically grooved seal modeled with a mass-conserving formulation, and extend the validity of the Reynolds model to account for inertia effect produced at the film discontinuity.

A significant number of numerical simulations were conducted, using either Reynolds+I code and CFD simulation software (OpenFoam), for different Reynolds number. The results showed a good agreement between the Re+I model and the NS model with a relative error that does not exceed 0.01 for all range of Reynolds number. Results also showed that the helix angle has a significant impact on the leakage and the same goes for the groove length to depth aspect ratio λ which also have a dramatic effect on the leakage that tends to be more prominent as the rotational speed increases.

A future work will further focus on the domain of validity of the modified Re+I model for helically grooved seal for different geometry configuration by comparing it to a 3D Navier Stokes model, and modified Re+I domain limit will be a subject of further study.

List of notations

D_h	Hydraulic diameter.
e_r	Relative error.
F	Switch function.
h	Film thickness.
h_d	Groove depth.
h_f	Clearance.
l_d	Groove width.
L	Viscoseal length.
p_{cav}	Cavitation pressure.
P_{NS}	Pressure obtained using NS model.
P_{Re+I}	Pressure obtained using Re+I model.

R	Viscoseal radius.
Re	Reynolds number.
v	Velocity of the outside surface.
β	Groove angle.
λ	Groove length to depth aspect ratio.
μ	Dynamic viscosity.
ξ	Pressure drop coefficient.
ρ	Density.

References

- [1] Arghir M, Alsayed A and Nicolas D 2002 The finite volume solution of the Reynolds equation of lubrication with film discontinuities *Int. J. Mech. Sci* **44** 2119–2132
- [2] Dobrica M B and Fillon M 2009 About the validity of Reynolds equation and inertia effects in textured sliders of infinite width *Proc Inst Mech Eng Part J: J. Eng. Tribol* **223** 69–78
- [3] Arghir M, Roucou M, Helene M and Frene J 2003 Theoretical analysis of the incompressible laminar flow in a macro-roughness cell *ASME J. Tribol* **125** 309–318
- [4] Dobrica M B and Fillon M 2005 Reynolds Model Suitability in Simulating Rayleigh Step Bearing THD Problems *Tribol. Trans* **48** 522–530
- [5] Sahlin F, Glavatskih F, Almqvist T R and Larsson R 2005 Two-dimensional CFD-analysis of micro-patterned surfaces in hydrodynamic lubrication *J. Tribol* **127** 96–102
- [6] Kumar A and Booker J F 1991 A finite element cavitation algorithm *ASME J. Tribol* **113** 276–284
- [7] Shi F and Paranjpe R 2002 An implicit finite element cavitation algorithm *Comput. Model. Eng. Sci* **3** 507–15
- [8] Bonneau D and Hajjam M 2001 Modélisation de la rupture et de la formation des films lubrifiants dans les contacts élastohydrodynamiques *Revue Européenne des Eléments Finis* **10** 679–704
- [9] Hajjam M and Bonneau D 2007 A transient finite element cavitation algorithm with application to radial lip seals *Tribol. Int* **40** 1258–69
- [10] Gherca A, Fatu A, Hajjam M and Maspeyrot P 2014 Effects of surface texturing in steady-state and transient flow conditions: Two-dimensional numerical simulation using a mass-conserving cavitation model *Proc. Inst. Mech. Eng. Part J: J. Eng. Tribol* **229** 505–22
- [11] Fatu A, Hajjam M and Bonneau D 2005 Analysis of non Newtonian and piezoviscous effects in dynamically loaded connecting-rod bearings *Proc. Inst. Mech. Eng. Part J: J. Eng* **219** 209–224
- [12] Fatu A, Hajjam M and Bonneau D 2005 An EHD model to predict the interdependent behaviour of two dynamically loaded hybrid journal bearings *ASME J. Tribol* **127** 416–424
- [13] Fatu A, Hajjam M and Bonneau D 2006 A new model of thermoelastohydrodynamic lubrication in dynamically loaded journal bearings *ASME J Tribol* **128** 85–95
- [14] Targaoui M, Souchet D and Bouyahia F 2015 On the hydrodynamic sealing in lubricated viscoseal *Tribology Transactions* **58** 527–536
- [15] Kanki K and Kawakami T 1987 Experimental study on the static and dynamic characteristics of screw Grooved seals *Rotating Machinery Dynamics* **1** 273–278
- [16] Ludwig L P, Strom T N, and Allen G P 1965 Experimental study of end effect and pressure patterns in helical groove fluid film seal (Viscoseal), *NASA Technical Note*, TN D-3096 Lewis Research Center, Cleveland, OH
- [17] Dai R X, Dong Q and Szeri A Z 1992 Approximations in hydrodynamic lubrication *ASME J. Tribol* **114** (1) 14–25
- [18] Dobrica M B and Fillon M 2006 Thermohydrodynamic behavior of a slider pocket bearing *ASME J. Tribol* **128** 312–318